



CHORUS

This is the accepted manuscript made available via CHORUS. The article has been published as:

Systematic study of symmetric cumulants at $\sqrt{s_{\text{NN}}}=200$ GeV in Au+Au collisions using a transport approach

Md. Nasim

Phys. Rev. C **95**, 034905 — Published 9 March 2017

DOI: [10.1103/PhysRevC.95.034905](https://doi.org/10.1103/PhysRevC.95.034905)

Systematic study of symmetric cumulants at $\sqrt{s_{NN}} = 200$ GeV in Au+Au collision using transport approach

Md. Nasim

University of California Los Angeles, CA 90095, USA

(Dated: February 22, 2017)

Measurement of 4-particle symmetric cumulants has been considered to be a good tool to study the correlations between amplitudes of different orders of anisotropic flow harmonics in the heavy-ion collision. These new observables not yet been measured at RHIC. Using A Multi-Phase Transport model, a set of predictions for the centrality dependence of the normalized 4-particle symmetric cumulants in Au+Au collisions at $\sqrt{s_{NN}} = 200$ GeV has been given. In addition, the effects of shear viscosity and hadronic rescattering on the magnitude of symmetric cumulants are discussed using AMPT model at $\sqrt{s_{NN}} = 200$ GeV. It is shown that $sc(2, 3)$ is found to be more sensitive to hadronic rescattering, whereas $sc(2, 4)$ is more sensitive to the shear viscosity. Rapidity dependence of symmetric cumulants is also shown. A relation between symmetric cumulant and event plane correlation is investigated using AMPT model.

PACS numbers: 25.75.Ld

I. INTRODUCTION

Elliptic flow (v_2) measured in heavy-ion collisions is believed to arise because of the pressure gradient developed when two nuclei collides at non-zero impact parameter followed by subsequent interactions among the constituents [1, 2]. If the nuclear overlap region were smooth, only even order flow harmonics (v_2, v_4, v_6 etc.) would be present in the final particle distributions. However, the nucleus is made up from a finite number of nucleons whose positions can fluctuate considerably event-by-event leading to fluctuations in the collision geometry [3]. These fluctuations could result in the production of odd order eccentricities in the initial geometry leading to formation of odd flow harmonics in the final particle distribution. The magnitude of v_n has been shown to be sensitive to the initial state and the equation of state of the system formed in the collisions [4]. Event-by-event measurement of anisotropic flow is crucial to understand the initial conditions in heavy-ion collision.

Correlations between different order flow harmonics are predicted to be sensitive to the transport properties of the produced medium in heavy-ion collisions. Recently, a new tool, namely 4-particle symmetric cumulants [5], is emerging with a promise to throw additional light on the initial-state phenomena and the transport properties of the produced medium in heavy-ion collisions [6–8].

The azimuthal distribution (ϕ) of particles in a given event is written as

$$P(\phi) = \frac{1}{2\pi} \sum_{n=-\infty}^{n=+\infty} V_n e^{-in\phi}, \quad (1)$$

where $V_n = v_n e^{in\psi_n}$ is the n^{th} harmonic anisotropic flow coefficient with respect to event plane angle ψ_n .

The 4-particle symmetric cumulants $SC(n, m)$ with $n \neq m$ [5] can be defined as

$$SC(n, m) \equiv \langle v_n^2 v_m^2 \rangle - \langle v_n^2 \rangle \langle v_m^2 \rangle. \quad (2)$$

Normalized symmetric cumulants $sc(n, m)$ is defined as

$$sc(n, m) \equiv \frac{\langle v_n^2 v_m^2 \rangle - \langle v_n^2 \rangle \langle v_m^2 \rangle}{\langle v_n^2 \rangle \langle v_m^2 \rangle}. \quad (3)$$

Magnitude of $sc(n, m)$ gives correlation strength between $\langle v_n^2 \rangle$ and $\langle v_m^2 \rangle$.

Recently, the ALICE collaboration has measured the $sc(2, 3)$ and $sc(2, 4)$ as a function of collision centrality [6]. This measurement has attracted an increased attention of many physicists, since a simultaneous description of v_n and $sc(n, m)$ cannot be captured using a single model with a constant initial condition and transport coefficient. Such measurement not yet been done at RHIC, leaving an opportunity to make predictions. In this paper, I made prediction of $sc(n, m)$ for upcoming measurements at RHIC as well as I have systematically studied the magnitude of $sc(n, m)$ under various condition using a transport model. This study will give a base line to understand the experimental data as well as a test of AMPT model which is very successful in describing magnitude of flow harmonics at RHIC energies.

This paper is organized in the following way. Section 2 describes details of the model used. In Section 3, transverse momentum spectra and magnitude of anisotropic flow harmonics of charged particle from AMPT model is presented. Comparisons with data and model are also shown. In Section 4, the effect of shear viscosity and hadronic re-scattering on the magnitude of $sc(n, m)$ are discussed. Rapidity de-

pendence of $sc(n, m)$ is also shown in Section 4. Sections 5 describes relation between $sc(n, m)$ and event plane correlation. Finally, I summarize in Section 5.

II. AMPT MODEL

The AMPT model is a hybrid transport model [9]. It uses the same initial conditions as in HIJING [10]. The AMPT model can be studied in two configurations, in the AMPT default version (AMPT-Def) in which the minijet partons are made to undergo scattering before they are allowed to fragment into hadrons [11], and in the AMPT string melting scenario (AMPT-SM) where additional scattering occurs among the quarks and hadronization occurs through the mechanism of parton coalescence. The string melting version of the AMPT model is based on the idea that for energy densities beyond a critical value of $\sim 1 \text{ GeV}/f\text{m}^3$, it is difficult to visualize the coexistence of strings (or hadrons) and partons. Hence, the need to melt the strings to partons. The scattering of the quarks is based on parton cascade [12]. In AMPT model, the value of parton-parton scattering cross-section, σ_{pp} , is calculated by

$$\sigma_{pp} \approx \frac{9\pi\alpha_s^2}{2\mu^2}, \quad (4)$$

where α_s is QCD coupling constant and μ is screening mass. In this study, approximately 5 M Au+Au events are generated for each configuration.

III. TRANSVERSE MOMENTUM SPECTRA AND ANISOTROPIC FLOWS FROM AMPT MODEL

Before I make a prediction using AMPT model, I need to fix set of input parameters by fitting experimental data on transverse momentum spectra and anisotropic flow harmonics. Figure 1 shows the transverse momentum (p_T) spectra of mid-pseudorapidity ($|\eta| < 0.5$) charged particles in different centrality bins. Black solid circles are data from STAR experiment [13] and open markers are AMPT model calculations with parton-parton interaction cross-section 1.5 mb and 3mb and default configuration. It is seen that AMPT model describe reasonably the experimental data at low p_T for all centralities. AMPT fails to describe data at high p_T ($> 1.5 \text{ GeV}/c$). This is due to the small current quark masses used in the AMPT model so that partons are less affected by the radial flow effect.

Now I show the transverse momentum dependence of charged particle $v_n(\psi_n)$ at mid-pseudorapidity ($|\eta| < 0.35$) in Au+Au collisions at $\sqrt{s_{NN}} = 200$

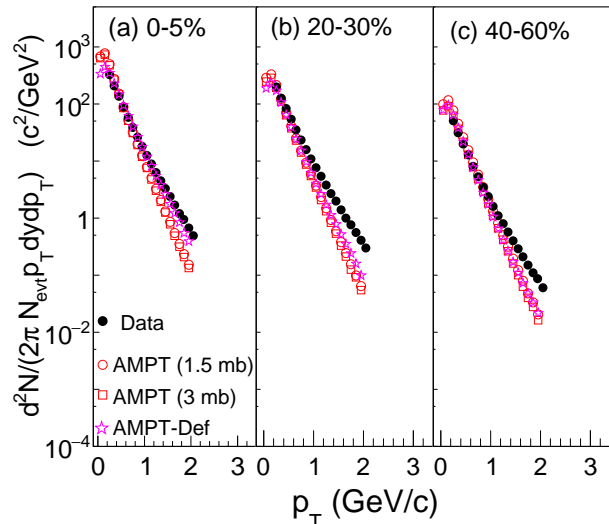


FIG. 1: (Color online) Transverse momentum spectra of charged hadron in Au+Au collision at $\sqrt{s_{NN}} = 200 \text{ GeV}$ for (a) 0-5% (most central) (b) 20-30% (mid-central) and (c) 40-60% (peripheral) centrality. Black solid circles are data [13] and open markers are AMPT model calculation.

GeV obtained from the AMPT model and its comparison with data, measured by PHENIX experiment [14]. Figure 2 shows comparison between data and AMPT model calculation for $v_2(\psi_2)$, $v_3(\psi_3)$ and $v_4(\psi_4)$, respectively. For v_n measurement in AMPT model, the azimuthal angle (ϕ) of each particle is correlated with event plane ψ_n^{avg} . Where ψ_n^{avg} is the average of ψ_n^{pos} and ψ_n^{neg} , calculated using charged particles within $1.0 < \eta < 2.8$ and $-2.8 < \eta < -1.0$, respectively (the same method as used in experimental data analysis [14]). Event plane resolutions in AMPT are comparable with the PHENIX data within the limit of 10%. It is seen from Fig. 2 that $v_n(\psi_n)$ measured by PHENIX can be described by using parton-parton cross-section between 1.5 to 3 mb. However, the agreement between data and model is not good for most central collisions. The AMPT model with default configuration predicts smaller v_n compared to AMPT with $\sigma_{pp} = 1.5$ and 3 mb.

IV. $sc(n, m)$ FROM AMPT MODEL

The magnitude of $v_n^2 v_m^2$ and v_n^2 in the numerator of Eq. 3 is calculated using multi-particle cumulant method [5] as shown below.

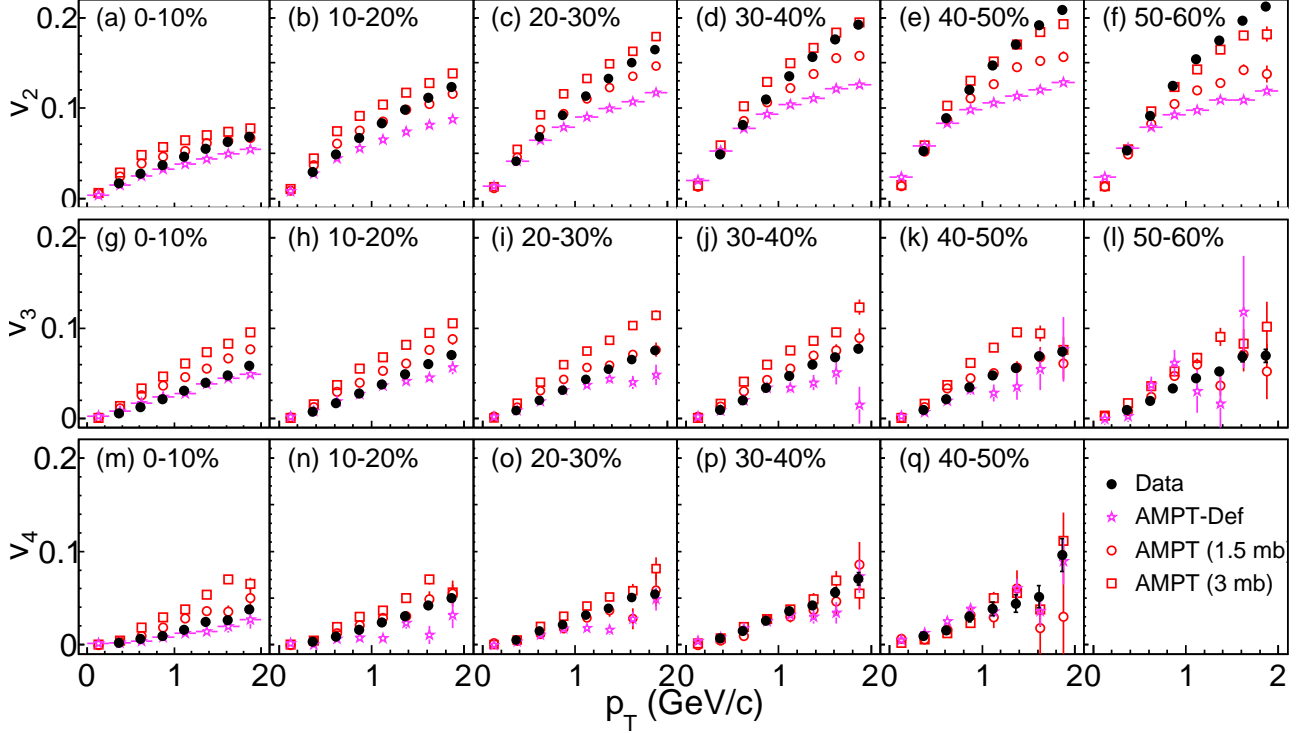


FIG. 2: (Color online) Transverse momentum dependence of v_2 , v_3 , and v_4 in Au+Au collision at $\sqrt{s_{NN}} = 200$ GeV for 0-10%, 10-20%, 20-30%, 30-40%, 40-50%, and 50-60% centrality. Black solid circles are data [14] and open markers are AMPT model calculation.

A. Hadronic vs. Partonic medium

$$\begin{aligned}
 v_n^2 v_m^2 &= \frac{1}{\binom{M}{4} 4!} \sum_{\substack{i,j,k,l=1 \\ (i \neq j \neq k \neq l)}}^M e^{i(m\varphi_i + n\varphi_j - m\varphi_k - n\varphi_l)} \\
 &= \frac{1}{\binom{M}{4} 4!} [|Q_m|^2 |Q_n|^2 - 2\Re [Q_{m+n} Q_m^* Q_n^*] \\
 &\quad - 2\Re [Q_m Q_{m-n}^* Q_n^*] + |Q_{m+n}|^2 + |Q_{m-n}|^2 \\
 &\quad - (M-4)(|Q_m|^2 + |Q_n|^2) + M(M-6)], \quad (5)
 \end{aligned}$$

and

$$v_n^2 = \frac{1}{\binom{M}{2} 2!} \sum_{\substack{i,j=1 \\ (i \neq j)}}^M e^{in(\varphi_i - \varphi_j)} = \frac{1}{\binom{M}{2} 2!} [|Q_n|^2 - M]. \quad (6)$$

Where M is the multiplicity of an event and Q_n is flow vector for n^{th} harmonic, $Q_n \equiv \sum_{k=1}^M e^{in\varphi_k}$. The weights of $M(M-1)$ and $M(M-1)(M-2)(M-3)$ are used to get the event-averaged 2-particle and 4-particle correlations. The magnitude of $\langle v_n^2 \rangle$ in the denominator of Eq. 3 is obtained with 2-particle correlations and using a pseudorapidity gap of $|\Delta\eta| > 1.0$ to suppress biases from few-particle non-flow correlations. Charged hadrons (π , K and p) within $0.2 < p_T < 2.0$ GeV/c and $|\eta| < 1.0$ are used in this analysis.

Measurement of $sc(n, m)$ has been done using both AMPT-SM (partonic medium) and AMPT-Def (hadronic medium) models keeping all other input parameters to be the same. The analysis was performed in 1% centrality bins, which are then recombined into 10% bins for reducing statistical uncertainty as suggested in ref [15]. Anti-correlation between v_2 and v_3 (Fig. 3a) and positive correlation between v_2 and v_4 (Fig. 3b) is observed for both AMPT-SM and AMPT-Def model. However (anti-) correlation strength between v_2 and (v_3 v_4) is stronger in the case of AMPT-def model which is a pure hadronic model. If there is any measurement of $sc(n, m)$ at BES energy at RHIC in future, this study could be useful to understand data.

B. Effect of shear viscosity

Transport coefficients play a major role in probing the properties of the medium created in high energy heavy ion collisions [16–23]. It has also been predicted that magnitude of $sc(n, m)$ could be sensitive

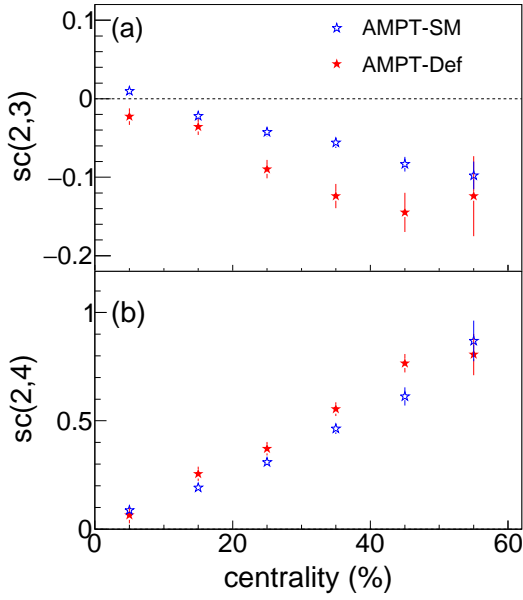


FIG. 3: (Color online) Centrality dependence of (a) $sc(2,3)$ and (b) $sc(2,4)$ in Au+Au collision at $\sqrt{s_{NN}} = 200$ GeV from AMPT-SM (blue) with $\sigma_{pp} = 3$ mb and AMPT-Def (red) model.

to the transport properties of the produced medium. In this paper, the magnitude of $sc(n, m)$ for different values of shear viscosity to entropy density ratio (η_s/s) using AMPT-SM model at $\sqrt{s_{NN}} = 200$ GeV is studied. For a system of massless quarks and gluons at temperature T ($T = 378$ MeV at RHIC energy in AMPT [24]), the η_s/s is given by [24]

$$\frac{\eta_s}{s} \approx \frac{3\pi}{40\alpha_s^2} \frac{1}{\left(9 + \frac{\mu^2}{T^2}\right) \ln\left(\frac{18 + \mu^2/T^2}{\mu^2/T^2}\right) - 18} \quad (7)$$

Three different value of η_s/s e.g. 0.08, 0.18 and 0.35 keeping $\alpha_s = 0.47$ are used in this study. It was shown that AMPT model with η_s/s between 0.18 ($\sigma_{pp} = 3$ mb) and 0.35 ($\sigma_{pp} = 1.5$ mb) explains magnitude of v_n . Fig. 4 shows centrality dependence of $sc(2,3)$ and $sc(2,4)$ in Au+Au collision at $\sqrt{s_{NN}} = 200$ GeV from AMPT-SM model. Black, red and blue marker corresponds to medium with $\eta_s/s = 0.35$, 0.18 and 0.08 respectively. The magnitude of $sc(2,4)$ increases with increase in shear viscosity, however anti-correlation between v_2 and v_3 decreases slightly with shear viscosity. Fig. 4 shows that the magnitude of $sc(2,4)$ is more sensitive to η_s/s compared to $sc(2,3)$. One can also finds that change in $sc(2,4)$ above $\eta_s/s = 0.18$ is negligible.

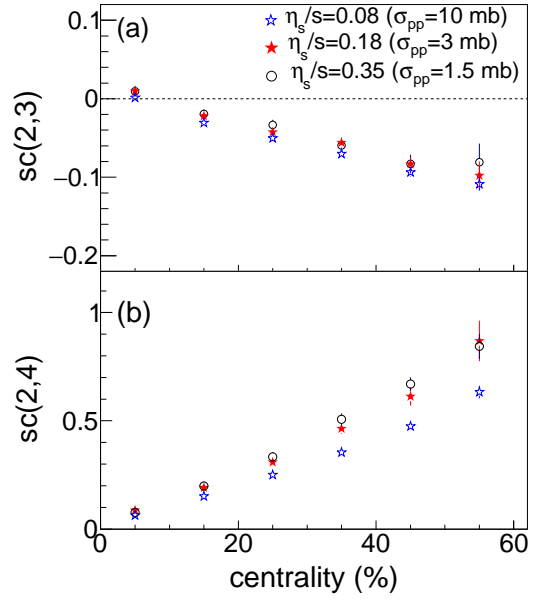


FIG. 4: (Color online) Centrality dependence of (a) $sc(2,3)$ and (b) $sc(2,4)$ in Au+Au collision at $\sqrt{s_{NN}} = 200$ GeV from AMPT-SM model for $\eta_s/s = 0.35$ (black), 0.18 (red) and 0.08 (blue).

C. Effect of hadronic re-scattering

The AMPT model with string melting leads to hadron formation using a quark coalescence model. The subsequent hadronic matter interaction is described by a hadronic cascade, which is based on a relativistic transport (ART) model [25]. The termination time of the hadronic cascade is varied in this paper from 0.6 to 30 fm/c to study the effect of the hadronic rescattering on $sc(n, m)$. Higher value of hadronic cascade time reflects larger hadronic rescattering. Fig. 5 shows centrality dependence of $sc(2,3)$ and $sc(2,4)$ in Au+Au collision at $\sqrt{s_{NN}} = 200$ GeV from AMPT-SM model with hadron cascade time = 0.6 fm/c (blue) and 30 fm/c (red). The magnitude of $sc(2,3)$ is found to be sensitive to hadron cascade time or hadronic rescattering. With increases in hadronic rescattering, the magnitude of $sc(2,3)$ decreases indicating more anti-correlation between v_2 and v_3 . On the other hand, change in $sc(2,4)$ due to change in hadron cascade time is negligible. Hence the correlation between v_2 and v_4 is not sensitive to the hadronic rescattering.

D. Rapidity dependence

In this section, rapidity dependence of $sc(n, m)$ is discussed. The different experiments have different detector setup with different rapidity coverage.

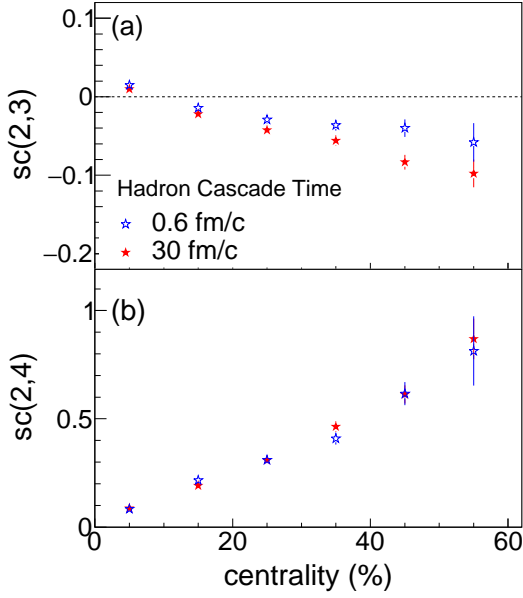


FIG. 5: (Color online) Centrality dependence of (a) $sc(2,3)$ and (b) $sc(2,4)$ in Au+Au collision at $\sqrt{s_{NN}}=200$ GeV from AMPT-SM model ($\sigma_{pp} = 3$ mb) for hadron cascade time = 0.6 fm/c (blue) and 30 fm/c (red).

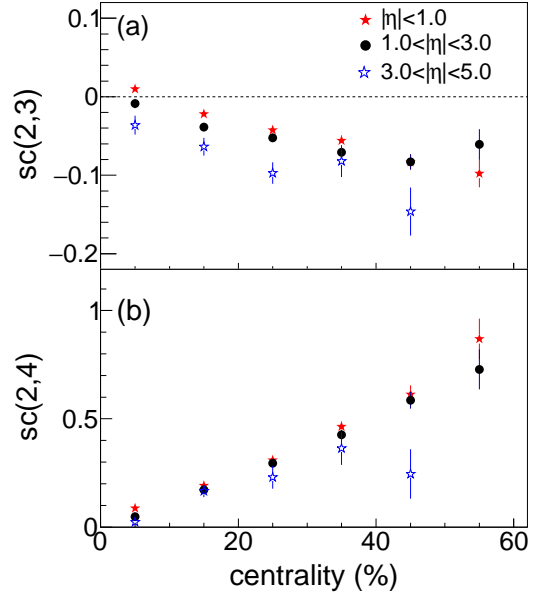


FIG. 6: (Color online) Centrality dependence of (a) $sc(2,3)$ and (b) $sc(2,4)$ in Au+Au collision at $\sqrt{s_{NN}}=200$ GeV from AMPT-SM model ($\sigma_{pp} = 3$ mb) with $|\eta| < 1.0$ (red), $1 < |\eta| < 3$ (black) and $3 < |\eta| < 5$ (blue).

Therefore, rapidity dependence of $sc(n, m)$ is studied to give a base line for future experimental measurement. Fig. 6 shows centrality dependence of $sc(2, 3)$ and $sc(2, 4)$ in Au+Au collision at $\sqrt{s_{NN}}=200$ GeV from AMPT-SM model with pseudo-rapidity coverage $|\eta| < 1.0$ (red), $1 < |\eta| < 3$ (black) and $3 < |\eta| < 5$ (blue). A change in magnitude of $sc(2, 3)$ and $sc(2, 4)$ for different pseudo-rapidity region is observed. Anti-correlation between v_2 and v_3 is stronger at far forward and backward pseudo-rapidity in comparison to mid-pseudo-rapidity. A strong positive correlation between v_2 and v_4 is observed at mid-pseudo-rapidity in comparison to far forward and backward pseudo-rapidity.

V. RELATION BETWEEN $sc(n, m)$ AND EVENT PLANE CORRELATION

In ref [26], authors derived a relation between $sc(n, m)$ and Event plane correlation and validity of this relation is tested using hydrodynamic calculation. Relation between $sc(2, 4)$ and correlation between 2nd and 4th order event plane ($\cos \Phi_{24}$) is shown in Eq. 8,

$$sc(2, 4) = \left(\frac{\langle v_2^6 \rangle}{\langle v_2^4 \rangle \langle v_2^2 \rangle} - 1 \right) \cos^2 \Phi_{24}, \quad (8)$$

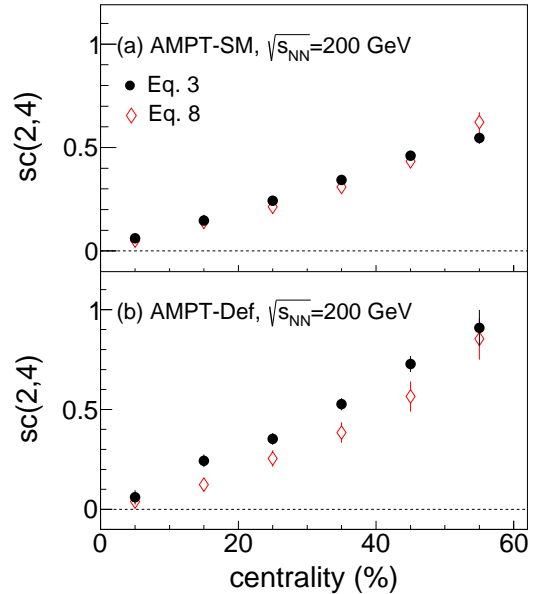


FIG. 7: (Color online) $sc(2,4)$ as a function of centrality from AMPT-SM ($\sigma_{pp} = 10$ mb) and AMPT-Def model in Au+Au collision at $\sqrt{s_{NN}}=200$ GeV. Black (Red) symbol represents calculation using Eq. 3 (Eq. 8)

where $\cos \Phi_{24} \equiv \frac{Re\langle V_4(V_2^*)^2 \rangle}{\sqrt{\langle v_2^2 \rangle \langle v_4^2 \rangle}}$. The magnitude of $\cos \Phi_{24}$ is measured using Eq. 9.

$$\cos \Phi_{24} = \frac{\langle Q_{2A}^2 Q_{4B}^* \rangle}{\sqrt{\langle Q_{4A} Q_{4B}^* \rangle} \sqrt{\langle Q_{2A}^2 Q_{2B}^* \rangle}}. \quad (9)$$

Here Q_{nA} and Q_{nB} are the n^{th} order flow vectors ($Q_n \equiv \sum_{k=1}^M e^{in\varphi_k}$) from two sub-event separated in pseudorapidity. No gap between two sub-events has been applied. The flow vectors Q_n is calculated using charged particle (π , K and p) within $0.2 < p_T < 2.0$ GeV/c and $0 < |\eta| < 1.0$. Eq. 8 relates 4-particle correlations ($sc(2,4)$) with 3-particle correlations (event-plane correlations) which is fully non trivial. It has been observed that event-by-event hydrodynamics satisfies Eq. 8 with a good approximation. Now, it is worth to check whether Eq. 8 is only valid in the hydro framework or it can be true in transport model too.

The magnitude of $sc(2,4)$ has been measured as a function of centrality using both Eq. 3 and Eq. 8 and comparison between them is shown in Fig. 7. Here the magnitude $sc(2,4)$ from Eq. 3 has been recalculated by recalculating v_n^2 in the denominator using 2-particle method with no pseudorapidity gap. This is done to make consistency between Eq. 3 and Eq. 8. Fig. 7(a) shows the comparison between Eq. 3 and Eq. 8 using AMPT-SM model in Au+Au collision at $\sqrt{s_{NN}}=200$ GeV. The ratio between red and black histograms is $\sim 20\%$ in AMPT-SM model. Fig. 7(b) shows comparison using AMPT-Def model. One finds that the deviation is larger in case of AMPT-Def (40%) compared to AMPT-SM (20%). I have also checked the validity of Eq. 8 by changing hadronic cascade time and magnitude of η_s/s , however, the conclusion remains the same. Therefore, Eq. 8 which relates 4-particle correlations with 3-particle correlations is not valid in hadronic transport model, like AMPT-Def. It has been shown in ref [26] that the event-by-event hydro model

satisfies Eq. 8. So, it is very important to check whether this relation is also valid in real data or not.

VI. SUMMARY

A set of predictions for the centrality dependence of the normalized symmetric cumulants in Au+Au collisions at $\sqrt{s_{NN}}=200$ GeV has been given using various configuration of AMPT model. AMPT-Def, which is a hadronic model, shows a stronger (anti-) correlation between v_2 and $(v_3)v_4$ compared to AMPT string melting model. Effect of the shear viscosity on the magnitude of symmetric cumulants ($sc(2,3)$ and $sc(2,4)$) is shown. The magnitude of $sc(2,4)$ and $sc(2,3)$ increases with increase in η_s/s . However, $sc(2,4)$ is more sensitive to η_s/s compared to $sc(2,3)$. The magnitude of $sc(2,3)$ is found to be sensitive with hadronic rescattering, whereas $sc(2,4)$ remains almost unaffected. The magnitude of $sc(2,3)$ decreases with increase in hadronic rescattering. Rapidity dependence of symmetric cumulants shows strong (anti)-correlation between v_2 and $(v_3)v_4$ at mid-rapidity compared to forward/backward rapidity. A non-trivial relation between symmetric cumulant and event plane correlation is tested in a transport-based AMPT model. String melting version of AMPT satisfy the relation, which connects symmetric cumulant and event plane correlation, with a better approximation compared to the AMPT-Def model(hadronic medium). These new observables have not yet been measured at RHIC. These study could be useful to understand upcoming measurements at RHIC.

Acknowledgments

Financial assistance from the Department of Energy, USA is gratefully acknowledged.

-
- [1] J. Y. Ollitrault, Phys. Rev. **D 46**, 229 (1992).
 - [2] H. Sorge, Phys. Rev. Lett. **78**, 2309 (1997).
 - [3] B. Alver and G. Roland, Phys. Rev. **C 81**, 054905 (2010).
 - [4] P. Huovinen *et al.*, Phys. Lett. **B503**, 58 (2001).
 - [5] A. Bilandzic *et al.*, Phys.Rev. **C 89**, 064904 (2014).
 - [6] J. Adam *et al.*, (ALICE Collaboration) Phys. Rev. Lett. **117**, 182301 (2016).
 - [7] X. Zhu *et al.*, arXiv:1608.05305.
 - [8] Y. Zhou *et al.*, Phys. Rev. **C 93**, 034909 (2016).
 - [9] Zi-Wei Lin and C. M. Ko, Phys. Rev. **C 65**, 034904 (2002);
Zi-Wei Lin *et al.*, Phys. Rev. **C 72**, 064901 (2005);
Lie-Wen Chen *et al.*, Phys. Lett. **B 605** 95 (2005).
 - [10] X. N. Wang and M. Gyulassy, Phys. Rev. **D 44**, 3501 (1991).
 - [11] B. Andersson *et al.* Phys. Rep. **97**,31 (1983).
 - [12] B. Zhang, Comput. Phys. Commun. **109**, 193 (1998).
 - [13] J. Adamset *al.* (STAR Collaboration), Phys. Rev. Lett. **91**, 172302 (2003).
 - [14] A. Adare *et al.* (PHENIX Collaboration), Phys. Rev. Lett. **107**, 252301 (2011).
 - [15] F. G. Gardim *et al.* arXiv:1608.02982.
 - [16] S. Chakrabarty, Pramana -J. Phys. **25**, 673 (1985).
 - [17] S. K. Das, V. Chanda, J. Alam, J.Phys. **G 41** 015102 (2013).
 - [18] A. K. Chaudhuri, Advances in High Energy Physics,

- vol. **2013**, Article ID 693180, (2013).
- [19] A. Nakamura and S. Sakai, Phys. Rev. Lett, **94**, 072305 (2005).
- [20] N. Demir and S. A. Bass, Phys. Rev. Lett., **102**, 172302 (2009).
- [21] H. Song and U. Heinz, J. Phys. **G 36**, 064033 (2009).
- [22] G. S. Denicol, T. Kodama, and T. Koide, Journal of Physics **G 37**, 094040 (2010).
- [23] R. Esha, M. Nasim, H. Z. Huang; arXiv:1603.02700.
- [24] J. Xu and C. M. Ko, Phys. Rev. **C 83**, 034904 (2011).
- [25] B.A. Li and C. M. Ko, Phys. Rev. **C 52**, 2037 (1995).
- [26] G. Giacalone *et al.* Phys. Rev. **C 94**, 014906 (2016).